Design optimization of lathe spindle system for optimum energy efficiency

Yi, Q., Li, C., Ji, Q., Zhu, D., Jin, Y., & Li, L. L. (2019). Design optimization of lathe spindle system for optimum energy efficiency. *Journal of Cleaner Production*, Article 119536. Advance online publication. https://doi.org/10.1016/j.jclepro.2019.119536

Published in:
Journal of Cleaner Production

Document Version:
Peer reviewed version

Design optimization of lathe spindle system for optimum energy efficiency

Qian Yi[a], Congbo Li[a,*], Qianqian Ji[a], Daoguang Zhu[a], Yan Jin[b], Lingling Li[c]

[a] *State Key Laboratory of Mechanical Transmission, Chongqing University, Chongqing 400044, China*

[b] *School of Mechanical and Aerospace Engineering, Queen's University Belfast, Belfast BT9 5AH, UK*

[c] *College of Engineering and Technology, Southwest University, Chongqing, 400715, China*

Abstract: Spindle system is the major mechanical component in machine tools, and its performance is responsible for a significant portion of the total consumed energy of machine tools. Conventional design optimization of spindle system is partially focused on parameter optimization of spindle motor or transmission system, contributing to an increase of the motor efficiency. Given that concurrent interactions among them is complex, very little efforts has been done to conduct integration optimization for optimum energy efficiency. To this end, a new approach of spindle system design is presented with consideration of the above two aspects adequately, to achieve the maximum energy and material efficiency. Firstly, the energy characteristic of spindle system is explicitly modeled on the basis of energy flow analysis. Then, a multi-objective optimization model for parameter optimization of spindle motor and transmission system is developed to take the both maximum energy efficiency and minimum volume as objectives, which is subjecting to a set of constraints with related to the cutting parameters boundary, processing requirements and shifting power losses. Finally, a multi-objective improved teaching-learning based optimization (MO-ITLBO) algorithm is presented to solve the developed optimization model. The performance of the proposed design approach of lathe spindle system is demonstrated through different working conditions. The experimental results indicate that the design of energy and material efficient machine tools can be achieved.

Key words: Design optimization; Lathe spindle system; Energy efficiency; Multi-objective optimization

1 Introduction

Manufacturing industry is extremely energy-intensive and accounts for about 37% of the world total energy use (IEA, 2017). Reducing energy consumption of manufacturing industry is an urgent and vital issue need to be solved due to global energy crisis and environment impacts. Among the various energy consumers of manufacturing industry, machine tools are the dominant energy consumers, which consume a substantial amount of energy but in low energy efficiency (Xiao et al., 2019). In the work reported by Gutowski et al. (2006), the energy efficiency of a typical milling process is only 14.8%. Hence, it is important and imperative to improve energy efficiency of the machine tools, which is crucial for the achievement of sustainable manufacturing and cleaner production (Wang et al., 2019).

Generally, there are two methods to improve the energy efficiency of machine tools. One is to design energy-efficient and material-efficient machine tools. Another is to optimize the machining process for energy saving (Chen et al., 2019; Xiao et al., 2019). Between these two methods, design of energy- efficient machine tool is recognized as a promising method to improve sustainability of machine tools in the design stage. To this end, in 2017, a standard published by the International Organization for Standardization (ISO) gives a framework of design method for energy-efficient machine tools (ISO 14955-1, 2017). It points out that the spindle system, feed system and auxiliary system of the machine tool are the main parts need to be optimized for energy saving. However, in this standard, there is a lack of detailed energy-efficient design approach for these parts. Usually, the spindle system of a machine tool is the major energy and material consumer. It consumes more

than 15% of the total energy of machine tools (Liu et al., 2018). Also, the spindle system might consume a substantial amount of material as it is manufactured. It is important for practitioners to explore the energy and material saving potentials of machine tools for sustainability considerations.

During the past decade, many researchers have been engaged in energy consumption analysis of the spindle system (Liu et al., 2012; Liu et al., 2015) as understanding energy consumption characteristic of the spindle system is the first step towards energy saving. Based on these works, some researchers began to investigate spindle motor optimization for energy efficiency improvement consideration. For example, Liu et al. (2017) developed a method to obtain the optimal working frequency and working torque of a motor, which can be used to select the spindle motors for high-efficiency spindle system design. Wójcicki and Bianchi (2018) studied the energy saving potentials of a spindle system of a computer numerical control (CNC) machine tool. Results of this study indicated that 10% energy consumption can be reduced by optimizing the spindle motor parameters such as the acceleration rate limit and the motor power limit. Liu et al. (2018) investigated that the spindle energy consumption was dependent on a specific motor and was useful in analyzing spindle motor efficiency for energy reduction. Chakkarapani et al. (2019) proposed a comprehensive framework of design optimization of motor parameters for maximizing output torque and minimizing total volume and total power losses to obtain the optimum geometric specifications of a motor.

Apart from the above studies about spindle motor optimization for energy efficiency improvement, another group of researchers focused on transmission system optimization to improve the energy efficiency of the spindle system, as the spindle system is usually consisted of motor and transmission system. Diez-Ibarbia et al. (2016) presented the influence of shifting profile effects on energy efficiency of spur gear transmissions. They revealed that a high shift coefficient resulted in a decrease in efficiency, in which the higher the torque, the lower the efficiency. Nejadkhaki et al. (2018) proposed a design method for selecting the optimal gear ratios. Simulation results indicated that energy efficiency of the transmission system can be increased the by around 5% by using their method. Miler et al. (2018) focused on the gearbox design with a goal of reducing the transmission power losses. Optimization results stated that the power losses decreased nearly 30%.

In recent years, minimization of the volume of machine tool structure starts to attract increasing research focuses for alleviating the material resource crisis. It is interesting to be noticed that the higher material efficiency in terms of smaller volume of machine structure always induces less energy consumption or higher energy efficiency. This is mainly because the smaller volume of the machine tool structure can induce less materials to fabricate the machine tool parts and less energy consumption demanded to operate the mass of materials. Mendi et al. (2010) performed a dimensional optimization of motion and force transmitting components of a gearbox for obtaining the smallest volume. Golabi et al. (2014) proposed a structure volume minimization method by selecting different gear ratio and gear hardness of gear trains. Experimental results showed that the structure volume of the gear train could be reduced by 7.8%. Zhang et al. (2018) studied optimization design on dynamic load sharing performance for an in-wheel motor speed reducer based on genetic algorithm. Case study showed that 2.81% of the structure volume could be reduced.

It is interesting to notice that the existing researches on design optimization of spindle system are mainly focused on either parameter optimization of spindle motor or parameter settings of transmission system. Very little work has comprehensively studied the concurrent interactions among spindle motor parameter settings and transmission system parameter design for both energy

and material savings. As reported by Waide and Brunner (2011), the energy consumption of spindle motor and transmission system might be reduced by around 20%-30% if the parameters of these two parts are tightly integrated. In addition to energy efficiency, different combinations of spindle motor and transmission system parameters also have a significant influence on the structure volume of the spindle system for material efficiency considerations.

Motivated by the above remarks, this paper attempts to fill this research gap and makes the following contributions. Firstly, a comprehensive energy consumption model of the spindle system is formulated by taking the parameters of both the spindle motor and the transmission system into consideration. Secondly, a multi-objective optimization model for minimizing specific energy consumption and minimizing structure volume is proposed and is solved via a multi-objective improved teaching-learning based optimization (MO-ITLBO) algorithm. The rest of the paper is organized as follows. The energy consumption model of spindle system is formulated in section 2. A multi-objective optimization model with a consideration of minimum specific energy consumption and structure volume and the MO-ITLBO algorithm are presented in section 3. In section 4, case studies are carried out to validate the proposed optimization method, followed by the conclusion and future research in Section 5. The framework of the proposed design optimization method for spindle system is depicted in Fig. 1.

Nomenclature

v_c	Cutting speed(m/min)	F_c	Cutting force(N)
f	Feed rate(mm/r)	$P_{Cu\text{-}p}$	Copper loss at peak point(W)
a_p	Cutting depth(mm)	$P_{Fe\text{-}p}$	Iron loss at peak point(W)
P_{in}	Input power of spindle system(W)	$P_{e\text{-}p}$	Eddy current loss at peak point(W)
P_c	Cutting power(W)	$P_{h\text{-}p}$	Hysteresis loss at peak point(W)
P_{loss}	Energy loss of spindle motor(W)	P_{max}	Peak power(W)
P_{Cu}	Copper loss (W)	P_N	Rated power(W)
P_{Fe}	Iron loss (W)	N_m	Maximum speed(rev/min)
P_e	Eddy current loss(W)	n_N	Rated speed(rev/min)
P_h	Hysteresis loss(W)	i_d	Low speed gear ratio
P_{mc}	Mechanical loss(W)	i_g	High speed gear ratio
P_{ad}	Additional load loss(W)	V_m	Spindle motor volume(m^3)
E_k	Kinetic energy of whole transmission components(J)	V_t	Gearbox volume(m^3)
		z_1	Gear teeth
E_m	Storage energy of electromagnetic field(J)	m_1	Gear modulus(mm)
E_{sp}	Energy consumption of spindle system(J)	b	Gear tooth width(mm)
V_{sp}	Volume of spindle system(mm^3)	ϕd	Tooth width coefficient
ω	Angular speed of motor shaft(rad/s)	k	Power loss ratio
α_1	Load loss coefficient of the mechanical transmission system	d	Workpiece diameter(mm)
		d_1	Spindle motor shaft diameter(mm)
α_m	Angular acceleration of spindle motor(rad/s^2)	d_2	Spindle shaft diameter(mm)
M	Spindle motor output torque(N.m)	$\cos\varphi$	Power factor
η	Machine tool efficiency	ρ	Conductor resistivity(Ω.m)
S	Conductor cross section(mm^2)	P_{SR}	Spindle rotation power(W)
L	Conductor length(mm)	f_{BA}	Basic frequency of the inverter(Hz)
U	Spindle motor voltage(V)	I	Spindle motor current(A)

h	Heat dissipation coefficient(W/m^2·K)	Δn	Speed range of power gap
A	Surface area of the motor core(mm^2)	J_s	Equivalent moment of inertia for motor shaft(kg.m^2)
t	Temperature rise limit(℃)		
t_A	Acceleration time preset in inverter(s)	p	The number of pole pairs of spindle motor
n_1	Initial spindle speed before acceleration(rev/min)	n_2	Final spindle speed after acceleration(rev/min)

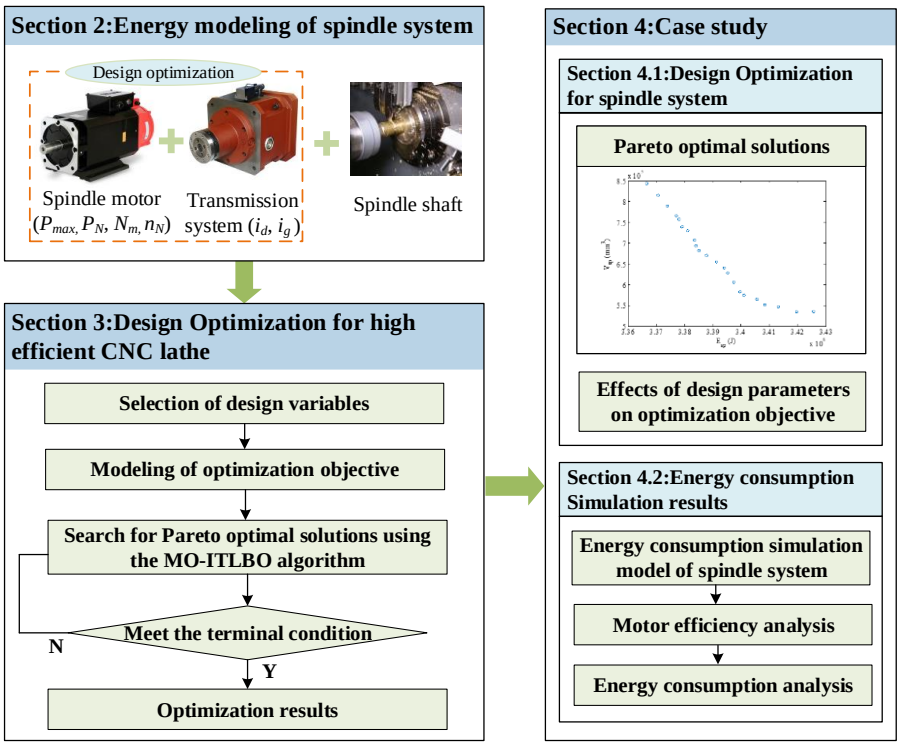

Fig. 1. Framework of design optimization for lathe spindle system

2 Energy modeling of spindle system

The energy behavior of spindle system is much complicated with dynamic changes. To predict the energy consumption related to motor and transmission parameters, this section presents the model framework of spindle system. The spindle system consists of the spindle motor, transmission system and spindle shaft. The spindle motor is the power source for machining. Its energy consumption is dynamically changed according to different cutting load. Usually, the spindle motor works around the rated speed to keep a relatively high efficiency. However, as most of the motor speed range is limited, this leads to a short time in working in the high efficiency region. To extend speed range of the spindle motor, a transmission system is applied to improve the efficiency of the motor. The energy flow of the spindle system of a typical CNC lathe is shown in Fig. 2.

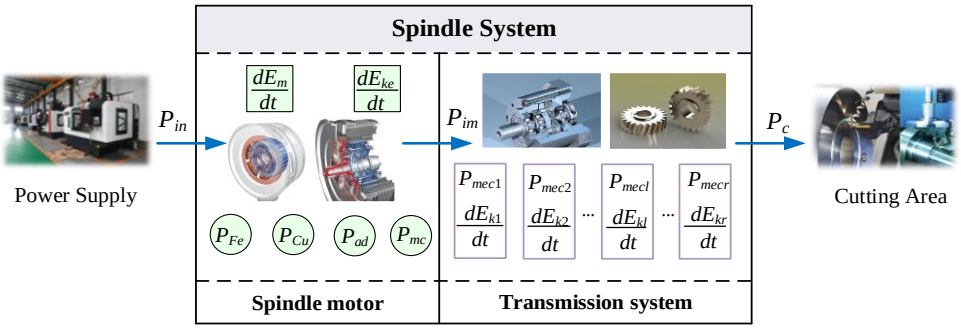

Fig. 2. Energy flow of the lathe spindle system

It can be found from Fig. 2 that when the electrical energy is transformed to mechanical energy by the spindle motor, there is a motor power loss. The motor power loss reduces the overall efficiency of the spindle system, resulting in a loss between the output power and input power of spindle motor. The relationship of the output power and the input power of spindle motor is shown in Eq. (1).

$$P_{in}(t)=\frac{P_{im}(t)}{\eta_m(t)} \tag{1}$$

where $P_{in}(t)$ is the input power of spindle motor at time t. $\eta_m(t)$ is the spindle motor efficiency at time t. $P_{im}(t)$ is the output power of spindle motor at time t.

2.1 Energy loss of spindle motor

According to the work presented by Wójcicki and Bianchi (2018), the energy efficiency of the spindle motor can be defined in Eq. (2).

$$\eta_m(t)=\frac{P_m(t)}{P_{loss}(t)+P_m(t)} \tag{2}$$

where $P_m(t)$ is spindle motor power at time t, and is expressed as $P_m(t)=N(t)\cdot M(t)/9550$, $N(t)$ is the motor speed at time t, $M(t)$ is the motor torque at time t. $P_{loss}(t)$ is energy losses of the spindle motor at time t, and consists of copper loss P_{Cu}, iron loss P_{Fe}, mechanical loss P_{mc}, and additional load loss P_{ad}. Iron loss includes eddy current loss P_e and hysteresis loss P_h.

The copper loss P_{Cu}, eddy current loss P_e and hysteresis loss P_h of the motor at any working point are related to the copper loss $P_{Cu\text{-}p}$, eddy current loss $P_{e\text{-}p}$ and hysteresis loss $P_{h\text{-}p}$ at the peak point, respectively. Mechanical loss P_{mc} and additional load loss P_{ad} can be obtained by empirical formulas. These power losses are defined by the following equations (Hall et al., 2001).

$$P_{Cu}=\begin{cases}[(n_N/N)(P_i/P_{\max})]^2 P_{Cu-p} & (N\le n_N)\\ (P_i/P_{\max})^2 P_{Cu-p} & (N>n_N)\end{cases} \tag{3}$$

$$P_e=\begin{cases}(N/n_N)^2 P_{e-p} & (N\le n_N)\\ P_{e-p} & (N>n_N)\end{cases} \tag{4}$$

$$P_h=\begin{cases}(N/n_N)P_{h-p} & (N\le n_N)\\ (n_N/N)^{0.6} P_{h-p} & (N>n_N)\end{cases} \tag{5}$$

$$P_{mc}=1.11\times10^{-5} N^{0.7}\cdot P_N \tag{6}$$

$$P_{ad}=0.064\cdot(P_{Cu}+P_e+P_h+P_{mc}) \tag{7}$$

where P_{max} is the peak power of the spindle motor, P_N is the rated power of the spindle motor, and n_N is the rated speed of the spindle motor.

The proportion of $P_{Cu\text{-}p}$ to $P_{loss\text{-}p}$ is 0.59, and the proportion of $P_{Fe\text{-}p}$ to $P_{loss\text{-}p}$ is 0.22. Both eddy current loss $P_{e\text{-}p}$ and hysteresis loss $P_{h\text{-}p}$ account for 0.5 of iron loss $P_{Fe\text{-}p}$. $P_{loss\text{-}p}$ is the motor total loss at peak point, which can be calculated by Eq. (8).

$$P_{loss-p} = \frac{2}{3} htA \tag{8}$$

where h is the heat dissipation coefficient, t is the limit of temperature rise, and A is the surface area of the motor core.

Thus, the relationships among the motor parameters (peak power, rated speed and rated power), motor working conditions (motor speed and motor torque) and motor efficiency can be obtained as follows:

When $N \le n_N$

$$\begin{aligned}\eta_m(t) = N(t)\cdot M(t)/9550 \Big/ \Big[\big(N(t)\cdot M(t)/9550\big) + \big(n_N \cdot M(t)/(9550\cdot P_{\max})\big)^2 \cdot P_{Cu-p} \\ + \big(N(t)/n_N\big)^2 \cdot P_{e-p} + \big(N(t)/n_N\big)\cdot P_{h-p} + 1.18\times 10^{-5}\big(N(t)\big)^{0.7}\cdot P_N \Big]\end{aligned} \tag{9}$$

When $N \ge n_N$

$$\begin{aligned}\eta_m(t) = N(t)\cdot M(t)/9550 \Big/ \Big[N(t)\cdot M(t)/9550 + \big(N(t)\cdot M(t)/(9550\cdot P_{\max})\big)^2 \cdot P_{Cu-p} \\ + P_{e-p} + \big(N(t)/n_N\big)^{0.6}\cdot P_{h-p} + 1.18\times 10^{-5}\big(N(t)\big)^{0.7}\cdot P_N \Big]\end{aligned} \tag{10}$$

2.2 Energy model of transmission system

The mechanical transmission system is an essential part for improving energy efficiency of machine tools. The energy consumption of the transmission system is consisted of three parts, i.e., friction energy, kinetic energy and cutting energy (Liu et al., 2012), which can be expressed in Eq. (11).

$$P_{im}(t) = P_{mec}(t) + \frac{dE_k(t)}{dt} + P_c(t) \tag{11}$$

where $E_k(t)$ is the kinetic energy of the mechanical transmission system at time t, $P_c(t)$ is the cutting power at time t. $P_{mec}(t)$ is the friction power at time t, and is composed of non-load power loss P_{um} and load power loss P_{am}, in which load power loss is linearly correlated with cutting power. The non-load power loss is given by Eq. (12).

$$P_{um}(t) = M_0\omega(t) + B(\omega(t))^2 \tag{12}$$

where $P_{um}(t)$ is the non-load power loss at time t, M_0 is the equivalent non-load Coulomb friction torque of the spindle system referred to the motor shaft, B is the equivalent viscous friction damping coefficient of the spindle system referred to the motor shaft, and $\omega(t)$ is the angular velocity of motor shaft at time t.

During the cutting process, the cutting power can be obtained according to the machining handbooks (Armarego et al., 2000), which is shown in Eqs. (13)-(14).

$$P_c(t) = F_c(t)v_c(t) \tag{13}$$

$$F_c(t) = C_{F_c} a_p^{x_{Fc}} f^{y_{Fc}} v_c^{n_{Fc}} K_{Fc} \tag{14}$$

where $F_c(t)$ is the cutting force at time t. a_p is the cutting depth. f is the feed rate. v_c is the cutting

speed. C_{Fc}, x_{Fc}, y_{Fc}, n_{Fc}, K_{Fc} are coefficients of the cutting force equation.

During the cutting process, the kinetic energy E_k is a constant. Hence, the change rate of the kinetic energy dE_k/dt is zero (Xie et al., 2016). Note that $v_c=\pi dn$, the input power of the transmission system can be calculated as shown in Eq. (15).

$$P_{im}(t) = 2\pi M_0 N(t) + 4\pi^2 B(N(t))^2 + \alpha_1 C_{F_c} a_p^{x_{F_c}} f^{y_{F_c}} K_{F_c} \left[\pi d N(t)/(1000\cdot i)\right]^{n_{F_c}+1} \tag{15}$$

where α_1 is the load loss coefficient of the mechanical transmission system, n is the spindle speed, d is the workpiece diameter, and i is the gear ratio.

3 Multi-objective optimization of spindle system

This section presents a multi-objective optimization model which takes the minimum specific energy consumption and minimum volume as objectives. The mathematical formulation of the two objectives is elaborated in Section 3.1. The design variables are defined and stratified in Section 3.2. The constraints involved in the optimization model are given in Section 3.3. Optimization solution via MO-ITLBO algorithm is introduced in Section 3.4.

3.1 Optimization objectives

In order to achieve high sustainable performance of machine tool, two objectives are considered for the design optimization problem, including 1) maximum energy efficiency of spindle system and 2) highest material efficiency in terms of minimum volume of spindle system.

3.1.1 Energy efficiency of spindle system

In this section, the energy efficiency of spindle system is evaluated in terms of the specific energy consumption (SEC_{sp}), which is defined as the ratio of the energy consumption of spindle system (E_{sp}) to material removal volume (MRV), in Eq. (16). The smaller the specific energy consumption, the higher the energy efficiency of spindle system.

$$SEC_{sp} = \frac{E_{sp}}{MRV} \tag{16}$$

$$E_{sp} = \int_0^t P_{in}(t)dt = \int_0^t \frac{P_{im}(t)}{\eta_m(t)}dt = \int_0^t \frac{2\pi M_0 N(t) + 4\pi^2 B(N(t))^2 + \alpha_1 C_{F_c} a_p^{x_{F_c}} f^{y_{F_c}} \left(\pi d N(t)\right)^{n_{F_c}+1} K_{F_c}}{\left(1000\cdot i\right)^{n_{F_c}+1}\eta_m(t)}dt \tag{17}$$

where t is working time of spindle system.

Given that $MRV=1000 v_c a_p f$, the specific energy consumption can be expressed as Eq. (18).

$$SEC_{sp} = \frac{E_{sp}}{MRV} = \int_0^t \frac{2\pi M_0 N(t) + 4\pi^2 B(N(t))^2 + \alpha_1 C_{F_c} a_p^{x_{F_c}-1} f^{y_{F_c}-1} \left(\pi d N(t)\right)^{n_{F_c}} K_{F_c}}{1000^{n_{F_c}+1} i^{n_{F_c}} \eta_m(t)}dt \tag{18}$$

3.1.2 Material efficiency of spindle system

In addition to improving material efficiency of spindle system, minimization of the volume of spindle system is considered as another optimization objective for maximum resource efficiency. The smaller the volume of spindle system, the higher the material efficiency of spindle system. The total volume of the spindle system is consisted of the volume of spindle motor and gearbox. Note that the volume of motor and gearbox shells are not considered in this paper because different types of motor and gearbox have different shapes. The volume of the spindle motor V_m is related to the volume of conductor, which can be expressed in Eq. (19).

$$V_m = SL \tag{19}$$

where S is the conductor cross section. L is the conductor length， which can be modelled in Eq.

(20).

$$L = \frac{US}{I\rho} \tag{20}$$

where U is the voltage of spindle motor. ρ is the resistivity of the conductor. I is the current of spindle motor, which is calculated as shown in Eq. (21) (Al-Badri et al., 2015).

$$I = \frac{P}{U \cdot \cos\varphi} \tag{21}$$

where P is the power consumption, $\cos\varphi$ is the power factor of the spindle motor.

For a machine tool, a two-stage transmission with high and low gear is usually developed to transmit power for different machining requirements. When a higher spindle torque is needed, the transmission system will shift to lower speed gear ratio to provide the desired torque. On the contrary, when a higher spindle speed machining is used, the transmission system will shift to higher speed gear ratio to increase the spindle speed. The volume of gearbox V_t is associated with the dimension of gears, which is defined in Eq. (22) (Golabi et al., 2014).

$$V_t = 0.25\pi b_1[(m_1 z_1)^2 + (m_1 z_1 i_d)^2 - d_1^2 - d_2^2] + 0.25\pi b_1[(m_2 z_2)^2 + (m_2 z_2 i_g)^2 - d_1^2 - d_2^2] \tag{22}$$

where m_1 and m_2 are gear modulus. z_1 and z_2 are gear teeth. b is gear tooth width, $b=\phi d \times d_g$, ϕd is tooth width coefficient and d_g is pitch circle diameter of gear. d_1 is the motor shaft diameter and d_2 is the spindle shaft diameter.

$$d_i \geq 1.64\sqrt{\frac{M_i}{[\varphi]}} \quad \forall i = 1, 2 \tag{23}$$

where $[\varphi]$ is the allowable torsion angle of the unit length of the shaft. M_i is the torque of motor shaft or spindle shaft.

By combing the Eq. (19)-(23), the spindle system volume function can be obtained, as expressed in Eq. (24). The smaller the volume V_{sp}, the higher the material efficiency of spindle system.

$$\begin{aligned} V_{sp} = V_m + V_t = {} & \frac{U^2 S^2 \cos\phi}{P_{\max}\rho} + 0.075\pi(m_1 z_1)^3(1+i_d^2) + 0.075\pi(m_2 z_2)^3(1+i_g^2) \\ & -0.225\pi(m_1 z_1 + m_2 z_2)\cdot\sqrt{k_1(N/i)^{n_{Fc}}(1+i)} \end{aligned} \tag{24}$$

3.2 Design variables stratification

Based on the analysis in Section 3.1, the spindle motor peak power P_{max}, rated power P_N, maximum speed N_m, rated speed n_N, low speed gear ratio i_d and high speed gear ratio i_g are selected as the design variables. However, the effects of design variables on optimization objectives are different. In order to investigate their influence relation, the sensitivity analysis is conducted to stratify the design parameters (Zhu et al., 2019).

The sensitivity of different design variables to the specific energy consumption and volume is calculated and plotted in Fig. 3. It can be seen that the specific energy consumption and volume are more sensitive to the changes of spindle motor peak power P_{max}, low speed gear ratio i_d and high speed gear ratio i_g than that of the other parameters such as rated power P_N, maximum speed N_m and rated speed n_N. Hence, the spindle motor peak power P_{max}, low speed gear ratio i_d and high speed gear ratio i_g are selected as high-sensitive parameters, while the other parameters are considered as low-sensitive parameters, in Table 1.

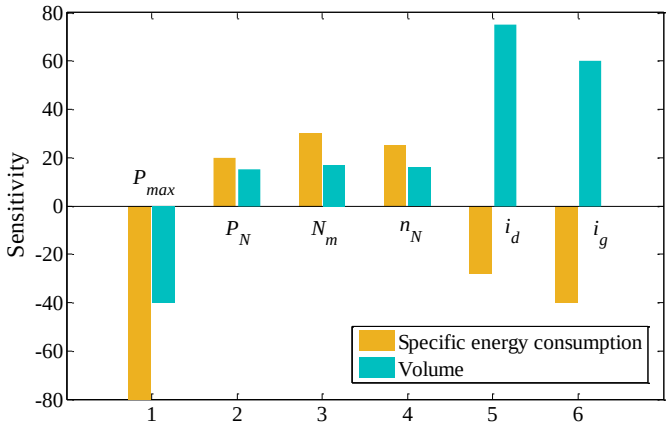

Fig. 3. Sensitivity analysis results of design parameters

Table 1. Results of parameters stratification

Parameters stratification	Design parameters
High-sensitive parameters	P_{max}, i_d, i_g
Low-sensitive parameters	P_N, N_m, n_N

The three-dimensional surface analysis is conducted to determine the optimization region of high-sensitive parameters, which lay the foundation for the MO-ITLBO algorithm. It can be seen from Fig. 4 that the interactions between high-sensitive parameters (P_{max}, i_d, i_g) and the two optimization objectives (SEC_{sp}, V_{sp}) are obtained. The variation range of three design parameters are further specified, which can significantly narrow parameter space, decrease the computational time and improve optimization efficiency.

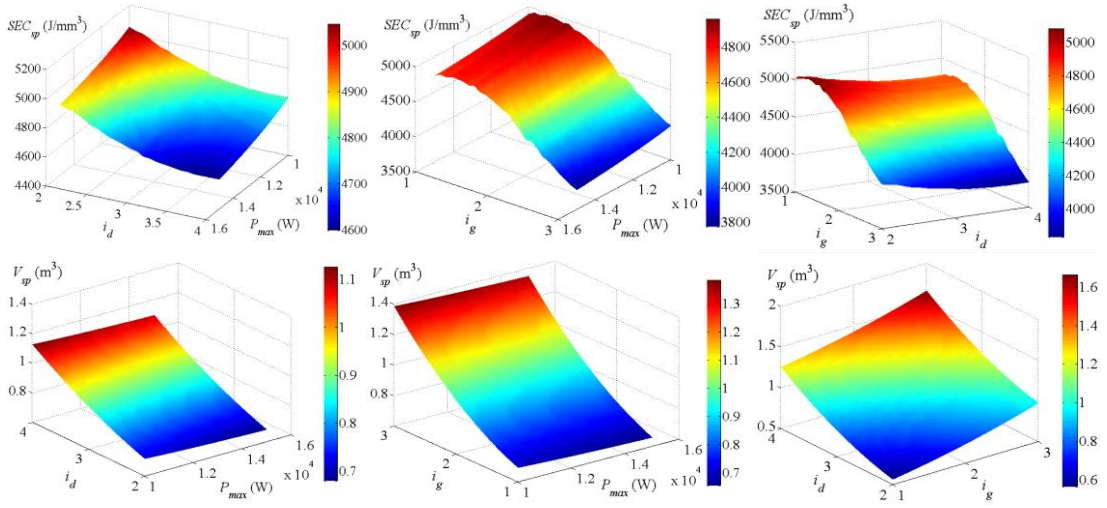

Fig. 4. Effects of high-sensitive parameters on optimization objectives

3.3 Constraints

The choice of design parameters should meet the processing requirements and mechanical properties of machine tool. The constraints set for the spindle system design problem are expressed as follows

a) A CNC lathe usually adopts a certain range of cutting parameters to ensure the machining capacity and to achieve the best dimensional tolerance. The commonly used cutting parameters could be obtained by considering tool material, workpiece material and the surface roughness to guarantee cutting efficiency, tool durability and machining quality. As the range of cutting

parameters plays an important role in designing the spindle system, this paper takes it as the basic condition for the optimization problem.

$$\begin{aligned} v_{c\min} \le v_c \le v_{c\max} \\ f_{\min} \le f \le f_{\max} \\ a_{p\min} \le a_p \le a_{p\max} \end{aligned} \tag{25}$$

b) The gear ratio must be in a specific range for the better mechanical characteristics and economy.

$$\begin{aligned} i_{d\min} \le i_d \le i_{d\max} \\ i_{g\min} \le i_g \le i_{g\max} \end{aligned} \tag{26}$$

where i_{dmin} and i_{dmax} are the minimum and maximum low speed gear ratio, i_{gmin} and i_{gmax} are the minimum and maximum high speed gear ratio.

c) The total power consumed by the spindle system should not exceed the maximum power provided by the spindle motor (Li et al., 2019).

$$C_{F_c} a_p^{x_{F_c}} f^{y_{F_c}} K_{F_c} \left(\pi dN / i\right)^{n_{F_c}+1} / \eta \le P_{\max} \tag{27}$$

d) The maximum acceleration power, which is consisted of power for spindle rotation and the power for overcoming the inertia of mechanical transmission system (Lv et al., 2017), should not exceed the rated power of spindle motor.

$$P_{SR} + \frac{\pi^2 f_{BA} J_s (n_2 - n_1)}{15 p t_A} + \frac{\pi^2 f_{BA}^2 J_s}{15 p t_A} \frac{N}{i} \le P_N \tag{28}$$

where P_{SR} is the spindle rotation power. f_{BA} is the basic frequency of the inverter. J_s is the equivalent moment of inertia for the spindle system referred to the motor shaft. p is the number of pole pairs of the spindle motor. t_A is the acceleration time preset in inverter. n_1 is the initial spindle speed before acceleration. n_2 is the final spindle speed after acceleration.

e) The spindle system adopts two-stage transmission with high and low speed gear ratio. The rated speed at high speed gear ratio is higher than the maximum speed at low speed gear ratio. When the transmission system shifts from high speed gear ratio to low speed gear ratio, the motor speed should be reduced lower than rated speed. The speed range is the constant torque region. The motor power increases linearly with the increment of motor speed in the region. As the motor power cannot be maximized, the power loss is produced in the shifting process, which is called power gap. The power gap should be stabilized within some limits in order to meet the usage requirement.

$$\frac{n_N i_d}{N_m i_g} \le k_{\max} \tag{29}$$

where k_{max} is maximum power gap.

f) During the shifting process, the power gap is generated in a specific motor speed range. The speed range of power gap should be minimized to guarantee the mechanical characteristics of the spindle shaft.

$$\frac{n_N}{i_g} - \frac{N_m}{i_d} \le \Delta n_{\max} \tag{30}$$

where Δn_{max} is the maximum speed range of power gap.

3.4 Optimization solution via MO-ITLBO algorithm

The proposed multi-objective optimization model is a strongly NP-hard problem with multi-objective, multi-constraint and multiple decision variables. In this section, the teaching-learning

based optimization (TLBO) algorithm is introduced to solve the proposed multi-objective optimization model. TLBO, which is first proposed by Rao et al. (2011), has been extensively used to deal with the mechanical design optimization problems due to the merits of efficient convergence rate and optimal solutions (Rao et al., 2011). The multi-objective improved teaching-learning based optimization (MO-ITLBO) algorithm is a multi-objective version of the basic TLBO presented by Patel and Savsani (2016). The algorithm simulates the traditional teaching-learning environment. The grades of the learners are improved by the teachers or other learners. The teachers are selected based on the Pareto-optimal mechanism to acquire high quality solutions with the consideration of multiple objectives.

In the proposed multi-objective optimization problem, there are a set of comprise solutions called Pareto optimal set to find a trade-off between the energy efficiency and material efficiency. If the energy efficiency and material efficiency of one learner are less than that of the other learner, the former learner will dominate the latter learner and become a non-dominated solution. Pareto optimal set refers to solutions that are not dominated by any single objective.

The flowchart of the MO-ITLBO algorithm is shown in Fig. 5. The main steps are elaborated in detailed below.

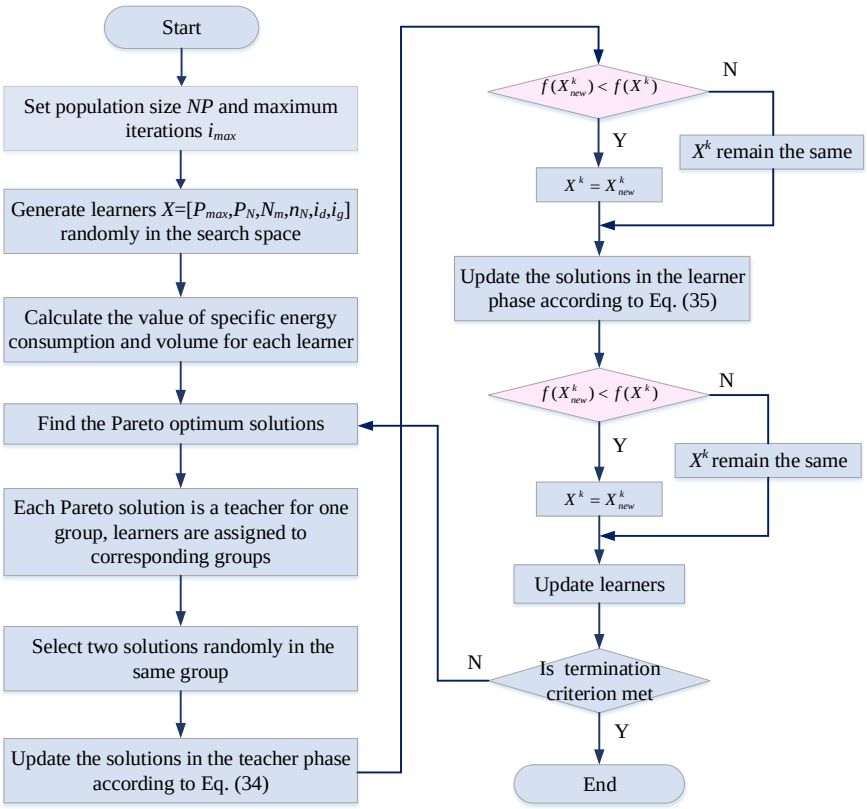

Fig. 5. Flowchart of the MO-ITLBO algorithm

3.4.1 Initialization of solution

The population consists of a large amount of learners, and every learner studies different subjects, which represents the different design variables for the optimization problem. The grades of the learners are the possible solutions, and the results of learners are the optimization objectives values. The potential solutions $X=[P_{max},P_N,N_m,n_N,i_d,i_g]$, i.e. the learners of the class, are represented by a six-dimensional vector $X= [x_{1,i}, x_{2,i}, \ldots, x_{j,i}]$, where j=1,2…,6 means the jth design parameter. Each

design parameter is generated randomly in the feasible range, as expressed in Eq. (31).

$$x_j = x_{j,L} + rand(0,1) \times (x_{j,U} - x_{j,L}),\ (j = 1,2,...,6) \tag{31}$$

where $x_{j,L}$ and $x_{j,U}$ are the upper and lower limits of design variables, respectively.

For each of the population, i.e., the six design parameters in matrix X, the feasibility are required to be checked whether the constraints in Eqs. (25)-(30) are satisfied. If a population does not satisfy the constraints, it is considered invalid and will be regenerated.

3.4.2 Generation of neighborhood solution

With the initial populations, the algorithm will obtain several group of non-dominated solutions where each non-dominated group refers to an individual Pareto front. In order to improve the diversity of populated solutions and further improve the global search ability, we use a two-phase neighborhood generation mechanism for each of the non-dominated group. The detailed procedure for generation of neighborhood solution based on an individual non-dominated group are given below.

(1) Teacher phase

In teacher phase, the learners improve their grades by studying from the teacher, who is the most knowledgeable person with optimal values of objective function. Learners with strong learning ability improve their grades quickly, while learners with weak learning ability improve grades slowly. Then, the mean results of each design parameter in the population is improved. The difference between the grade of the teacher and mean grade of the learners in each subject is expressed as Eq. (32).

$$difference\_Mean^s_{k,j,i} = r_i (X^s_{b,j,i} - (T_F)^s_{k,i} \times M^s_{j,i}) \tag{32}$$

where $X^s_{b,j,i}$ is the grade of the teacher associated with group 's' in subject 'j' at iteration 'i', that is the six design parameters. $M^s_{j,i}$ is the mean grades of the group 's'. T_F is the teaching factor. Every student adopts an adaptive teaching factor, which is determined by the optimization objective values of the student, as expressed in Eq. (33).

$$(T_F)^s_k = \begin{cases} \dfrac{f(X^k)}{T_s}, T_s \neq 0 \\ 1 \quad , T_s = 0 \end{cases} \tag{33}$$

where $f(X^k)$ is the normalized objective function related to the specific energy consumption and volume with learner 'k'. T_s is the optimal objective value of the teacher in group 's'.

Learners can improve themselves not only through learning from the teacher, but also through discussing with other learners. A learner randomly selects another student and analyzes the results of normalized objective function to conduct selective learning, which is updated through the expression as Eq. (34).

$$\begin{aligned} X^s_{k,j,i,new} &= X^s_{k,j,i} + difference\_Mean^s_{k,j,i} + r_i (X^s_{h,j,i} - X^s_{k,j,i}), \quad f(X^s_h) < f(X^s_k) \\ X^s_{k,j,i,new} &= X^s_{k,j,i} + difference\_Mean^s_{k,j,i} + r_i (X^s_{k,j,i} - X^s_{h,j,i}), \quad f(X^s_k) < f(X^s_h) \end{aligned} \tag{34}$$

where X^s_k is the original sequence of design parameters with learner 'k', and $X^s_{k,new}$ is the new sequence of design parameters. If $X^s_{k,new}$ has smaller objective values than X^s_k, it will be accepted as the new solutions. r_i is the random number in the range [0,1].

(2) Learner phase

All the accepted grades of each learner (optimization variables) are maintained at the end of the

teacher phase and these values become the input to the learner phase. In the learner phase, the learners interacts with other learners for acquiring more knowledge. On the other hand, the learners consider to enhance knowledge through self-learning. The search direction of the learner is determined by comparing to other learners' results, and the new grades of the learner can be obtained. The search mechanism that the learners acquire knowledge without teacher's help is incorporated in the learner phase, which is expressed in Eq. (35).

$$\begin{aligned} X^s_{p,j,i,new} &= X^s_{p,j,i} + r_i(X^s_{p,j,i} - X^s_{q,j,i}) + r_i(X^s_{b,j,i} - (E_F)_i X^s_{p,j,i}), \quad f(X^s_p) < f(X^s_q) \\ X^s_{p,j,i,new} &= X^s_{p,j,i} + r_i(X^s_{q,j,i} - X^s_{p,j,i}) + r_i(X^s_{b,j,i} - (E_F)_i X^s_{p,j,i}), \quad f(X^s_q) < f(X^s_p) \end{aligned} \tag{35}$$

where p and q are the learners in the group 's'. E_F is the exploration factor and its value is determined randomly by $E_F=round(1+r_i)$.

The grades of the learner is updated by selecting other learners randomly. The new learner will be accepted if it gives a better results.

4 Case study

In this section, the necessity of the multi-objective optimization approach is first analyzed under different case study settings. The influence of the design parameters on the two optimization objectives are also analyzed. The energy saving performance of the proposed design approach is further demonstrated through a simulation model where the energy consumption of machine tools are monitored under the different working conditions.

4.1 Design Optimization for spindle system

4.1.1 Optimization results

In this section, the machining experiments are performed on a CNC lathe C2-6150HK provided by Chongqing No.2 MT works Co., Ltd, China. The structure of the lathe is shown in Fig. 6. Table 2 provides the specifications of the process parameters, spindle motor and transmission system.

Table 2. Specifications of the process parameters, spindle motor and transmission system

Item	Unit	Numerical data
Machine tool		
Cutting speed	$[v_{c\,min}, v_{c\,max}]$(m/min)	[80, 200]
Feed rate	$[f_{min}, f_{max}]$(mm/r)	[0.1, 2]
Cutting depth	$[a_{p\,min}, a_{p\,max}]$(mm)	[0.1, 3]
Maximum workpiece diameter	d_{max}(mm)	250
Spindle motor		
Peak power	P_{max}(W)	11000
Rated power	P_N(W)	7500
Maximum speed	N_m(rev/min)	3000
Rated speed	n_N(rev/min)	1450
Transmission system		
Low speed gear ratio	i_d	2.75
High speed gear ratio	i_g	1.64

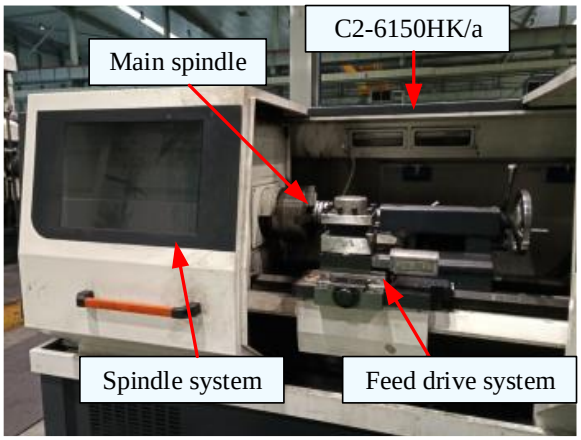

Fig. 6. Mechanical system of C2-6150HK/a CNC lathe

In order to demonstrate the necessity of the proposed multi-objective optimization approach, three cases are designed as follows. Case 1 is a single-objective optimization problem where Minimum SEC_{sp} is taken as an objective for the integrated optimization of spindle motor parameters and transmission system parameters. Case 2 uses the same integrated optimization strategy but with a different optimization objective, i.e., Minimum V_{sp}. Case 3 is a multi-objective integrated optimization problem to take both the minimum SEC_{sp} and the minimum V_{sp} as objectives. It should be noted that the three cases are carried out under the same working conditions (with identical cutting speed, feed rate and cutting depth). For the single-objective optimization (i.e., Case 1 and Case 2), the traditional ITLBO algorithm is conducted to obtain the optimal parameters for both the spindle motor and transmission system. The multi-objective optimization (i.e., Case 3) is solved via the MO-ITLBO. The Pareto front of Case 3 is shown in Fig. 7 and the circle marked in blue represents the Pareto optimum solutions.

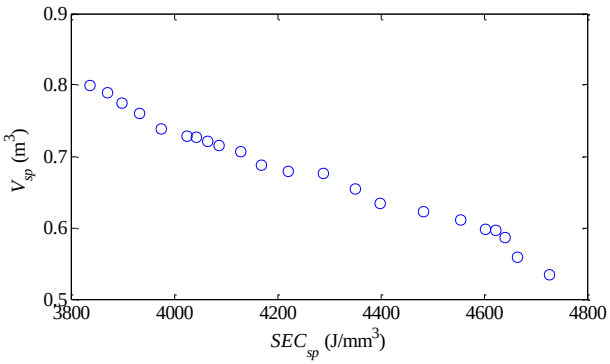

Fig. 7. Pareto optimum solutions of the multi-objective optimization

The optimization results of the three cases are shown in Table 3. It is clear from Table 3 that the optimization results of single-objective (Case 1 and Case 2) reveal that the lower specific energy consumption accompanies the higher volume, and the higher specific energy consumption follows the lower volume. Apparently, the energy-oriented design optimization does not yield a solution that meets the requirement of miniaturization. The multi-objective optimization method can achieve a trade-off between minimum specific energy consumption and minimum volume. It is clear from Table 3 that Case 3 decreases the specific energy consumption by 16.58% compared to Case 2 and decreases the volume by 8.59% compared to Case 1. Therefore, the proposed multi-objective integration method which can simultaneously minimum specific energy consumption and minimum volume has practical significance.

Table 3. Optimization results

Optimization objective	P_{max}(W)	P_N(W)	N_m(rev/min)	n_N(rev/min)	i_d	i_g	SEC_{sp}(J/mm^3)	V_{sp}(m^3)
Minimum SEC_{sp}	14993	7133	2742	1016	2.53	2.0	3726.4	0.7975
Minimum V_{sp}	15000	7075	3255	1256	2.0	1.0	4825.3	0.5292
Minimum SEC_{sp}&V_{sp}	14928	9266	3250	1000	2.37	1.81	4025.2	0.7290
Original parameters	11000	7500	3000	1450	2.75	1.64	4832.4	0.8238

Motor efficiency can be also calculated to verify the optimization results according to the cutting parameters boundaries in the CNC lathe. The detailed results are shown in Fig. 8. It is clear from Fig. 8 that the optimized spindle system makes the spindle motor work in higher efficiency region as much as possible, and the high-efficient region of spindle motor is enlarged. The spindle motor working in efficiency region 0.8~0.85 is raised to 0.85~0.9, resulting in less energy consumption of spindle system. In addition, with the optimized design parameters the volume of spindle system is also calculated according to Eq. (24). The results show that the spindle system volume has reduced from 0.8238m^3 to 0.7290m^3, which is decreased by 11.51% and makes the structure compact.

A spindle motor with appropriate size avoids excessive volume and saves production cost. A shiftable gearbox with minimum volume design is employed to meet required spindle speed and torque, which takes less material costs. The motor working conditions (motor speed and motor torque) are obtained through the spindle working conditions and gear ratio. When the motor working conditions are acquired, the motor efficiency can be calculated according to Eqs. (9) and (10). It is of great significance to design high efficiency motors for energy-efficient machine tools.

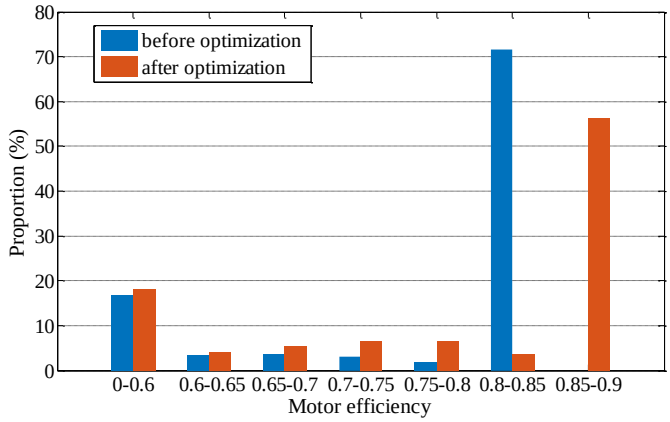

Fig. 8. Proportion of motor efficiency in the cutting parameters boundaries

4.1.2 Effects of design parameters on optimization objectives

The influence of the design parameters on the specific energy consumption and the volume is depicted in Fig. 9 and Fig. 10, respectively. It can be seen that both the specific energy consumption and the volume decrease with the raise of peak power. As the rated power and maximum speed increase, the specific energy consumption increases while the volume keeps unchanged. The specific energy consumption increases, but the volume decreases with the raise of rated speed. As the low speed gear ratio and high speed gear ratio increase, the specific energy consumption decrease while the volume increase.

The specific energy consumption is decreased when a large peak power, low speed gear ratio, high speed gear ratio, as well as a small rated power, maximum speed and rated speed are selected. However, the volume will be decreased when choosing a large peak power and rated speed, as well as a small low speed gear ratio and high speed gear ratio. According to Table 3, the low speed gear

ratio and high speed gear ratio of Case 1 (for minimization of specific energy consumption) is much higher than that of Case 2 (for the minimization of the volume). However, the rated speed of Case 2 (for minimization of the volume) is much higher than that of Case 1 (for minimization of specific energy consumption). For Case 3 with both minimum SEC_{sp} and minimum V_{sp}, the values of rated speed, low speed gear ratio and high speed gear ratio strike a balance between those in the single-objective optimization cases (i.e., Case 1 and Case 2). Moreover, the peak power should be higher, rated power and maximum speed should be lower in the permitted ranges.

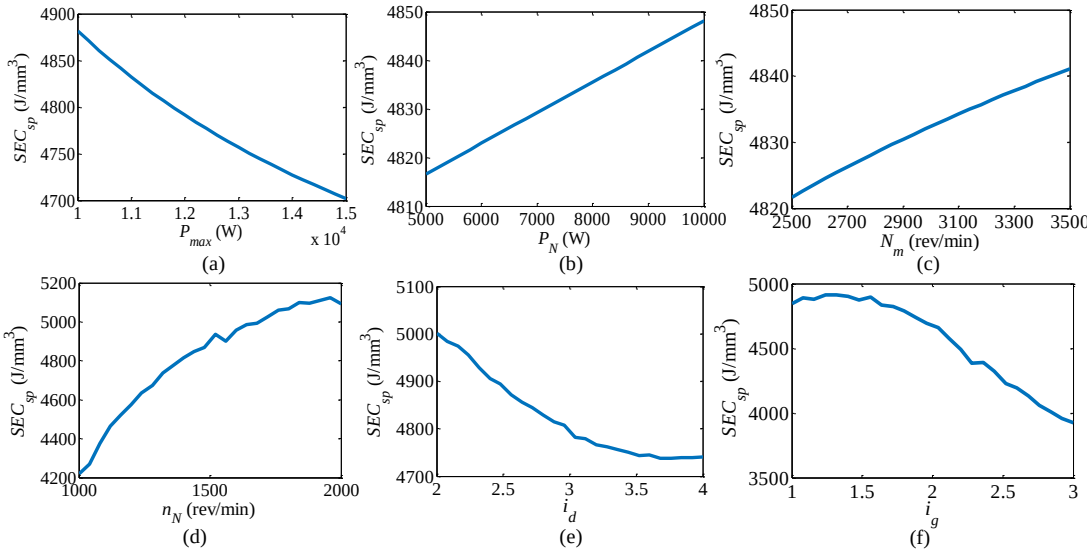

Fig. 9. Specific energy consumption changes with respect to a) peak power b) rated power c) maximum speed d) rated speed e) low speed gear ratio f) high speed gear ratio

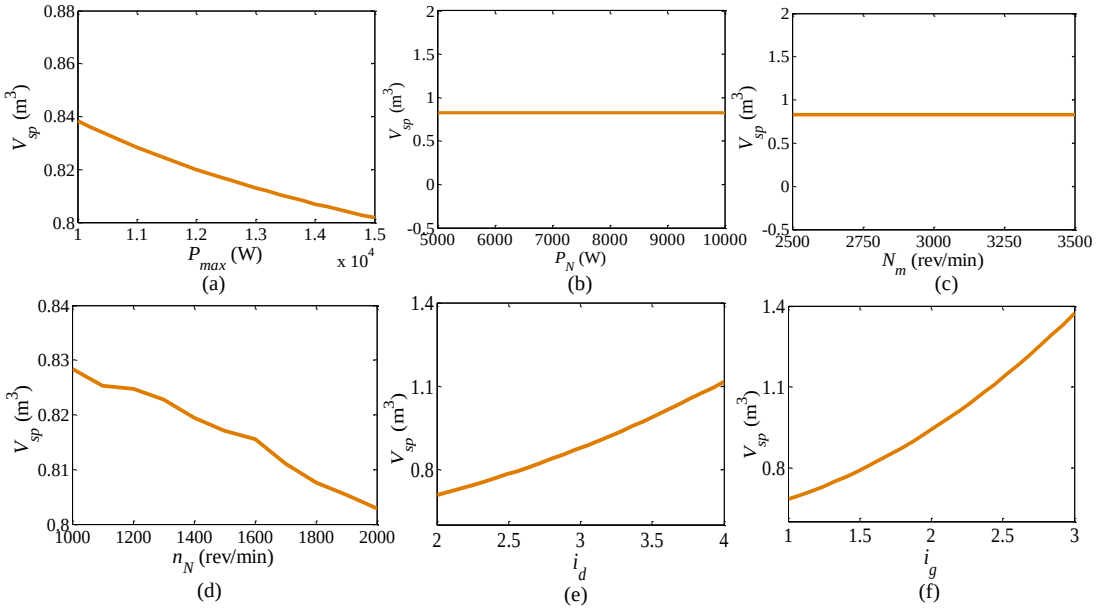

Fig. 10. Volume changes with respect to a) peak power b) rated power c) maximum speed d) rated speed e) low speed gear ratio f) high speed gear ratio

4.2 Energy consumption simulation results

Given that specific machined parts with constant process parameters have the same material removal volume, the specific energy consumption is replaced by the energy consumption, which can be calculated through simulation experiments. The energy consumption simulation model of

the spindle system is established with the MATLAB/Simulink. The simulation model includes the working condition model, the transmission system model, the spindle motor model and the energy consumption monitor model, in Fig. 11. These models are developed to calculate the energy consumption for machining a workpiece. In the working condition model, the spindle speed and torque are computed through the cutting parameters, and transmitted to the transmission system model. The spindle motor speed and torque can be obtained through the transmission relationship. Followed by spindle motor model, motor speed and torque are used to calculate the motor output power and motor efficiency, which are conducted to acquire the real-time input power of spindle motor. The integral of real-time input power and time is the energy consumption of the spindle system, which can be obtained through energy consumption monitor model.

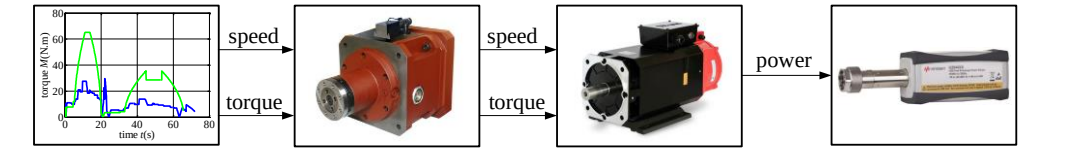

Fig. 11. Energy consumption simulation model of spindle system

(1) Working condition model

Two different working conditions are designed for CNC lathe machining tests, i.e., camshaft and input shaft. The drawings of the two parts indicate the structure, dimensions and processing requirements of each workpiece, Fig. 12 and Fig. 13, respectively. The operation is divided into roughing and finishing, and the process includes cylindrical and face turning. The working condition data is derived from the actual machining parameters.

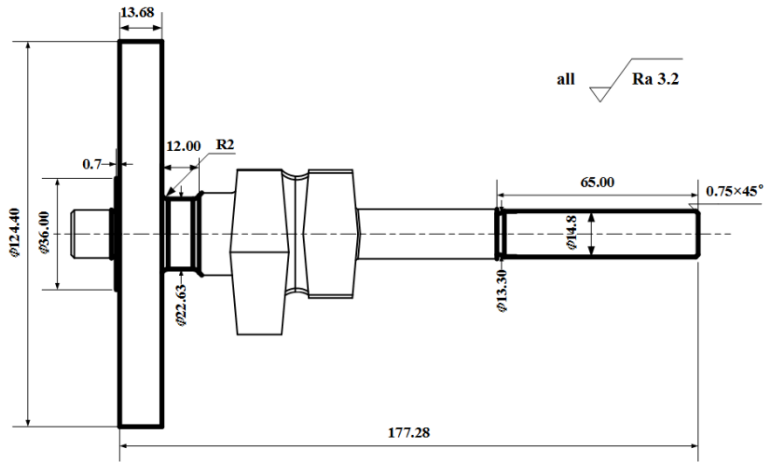

Fig. 12. Camshaft part drawing

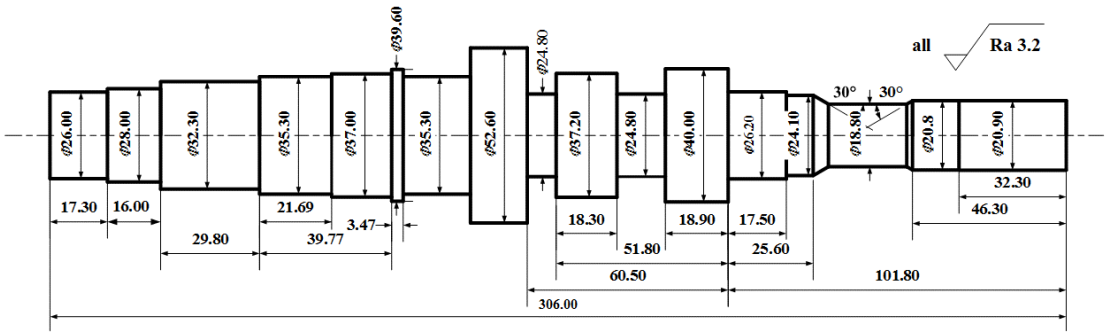

Fig. 13. Input shaft part drawing

The data about the machining condition and related parameters are given in Table 4, 5 and 6.

Table 4. Working conditions for turning

Tool material	Workpiece	Workpiece material
Cemented carbide	Camshaft	45#steel
Cemented carbide	Input shaft	45#steel

Table 5. Calculation coefficients of cutting force

Influence coefficient of force	Value	Exponential coefficient of cutting depth	Value	Exponential coefficient of feed rate	Value	Exponential coefficient of cutting speed	Value	Correction coefficient	Value
C_{Fc}	2648	x_{Fc}	1.0	y_{Fc}	0.75	n_{Fc}	-0.15	K_{Fc}	1.0
C_{Fp}	1952	x_{Fp}	0.9	y_{Fp}	0.6	n_{Fp}	-0.3	K_{Fp}	1.0
C_{Ff}	2884	x_{Ff}	1.0	y_{Ff}	0.5	n_{Ff}	-0.4	K_{Ff}	1.0

Table 6. Calculation parameters of lathe spindle system

Item	Notation	Value
Spindle motor voltage	U (V)	380
Power factor	$\cos\varphi$	0.83
Gear module	m(mm)	3
Gear teeth	z_1	22
Gear teeth	z_2	30
Tooth width coefficient	ϕd	0.3
Allowable torsion angle	[φ] (°/m)	0.8
Cross section of conductor	S(mm^2)	4
Conductor resistivity	$\rho(\Omega \cdot mm^2/m)$	0.0175
Basic frequency of the inverter	f_{BA}(Hz)	50
Initial spindle speed	n_1(rev/min)	0
Final spindle speed	n_2(rev/min)	3000
Acceleration time preset in inverter	t_A(s)	3
The number of pole pairs of motor	p	2

The cutting parameters of machine tool are used to calculate the spindle speed and torque according to the equations n=1000v_c/(πd) and T=Fd/2. In this section, two workpieces (i.e., a camshaft and an input shaft) are taken as metal cutting materials for machining experiments. The spindle speed and torque curves when machining camshaft and input shaft are shown in Fig. 14 and Fig. 15, respectively. The speed and torque are taken as input working conditions for the simulation model.

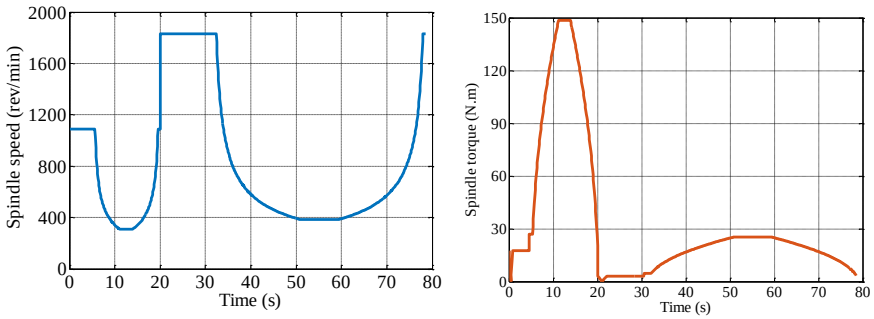

(a) (b)

Fig. 14. a) spindle speed and b) spindle torque for machining camshaft

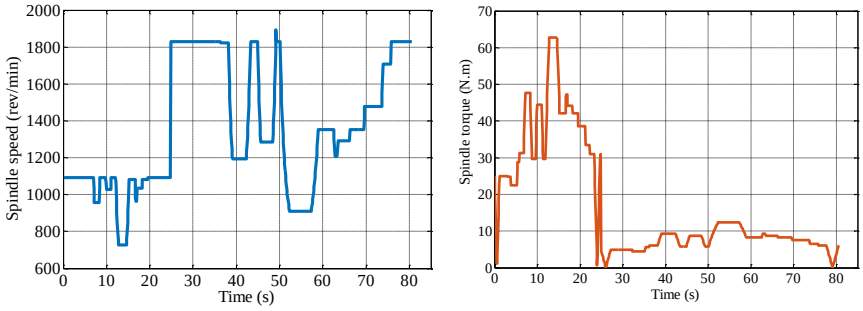

(a) (b)

Fig. 15. a) spindle speed and b) spindle torque for machining input shaft

(2) Transmission system model

The function of the transmission system model is to convert the spindle speed and torque into the spindle motor speed and torque. The transmission system simulation model is shown in Fig. 16, where *fd_ratio*1 is the low speed gear ratio and *fd_ratio*2 is the high speed gear ratio. When the low speed gear ratio or high speed gear ratio is selected, the corresponding spindle motor speed and torque are output. When neutral gear is selected, the output speed and torque of spindle motor are zero.

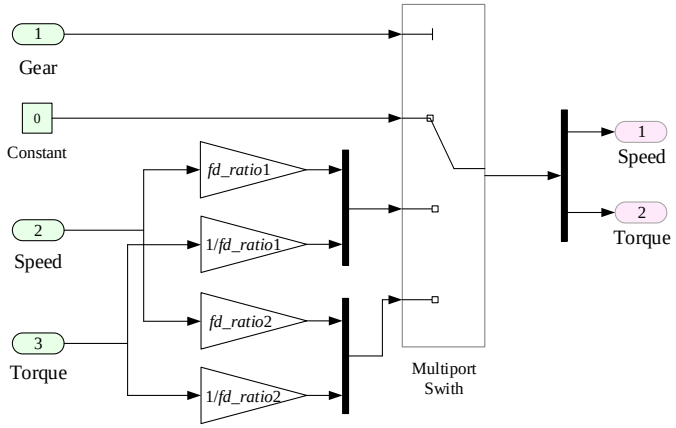

Fig. 16. Transmission system simulation model

(3) Spindle motor model

The spindle motor simulation model is shown in Fig. 17. The function of the simulation model is to transform the motor speed and torque into the motor output power and motor efficiency for computing the input power of spindle motor.

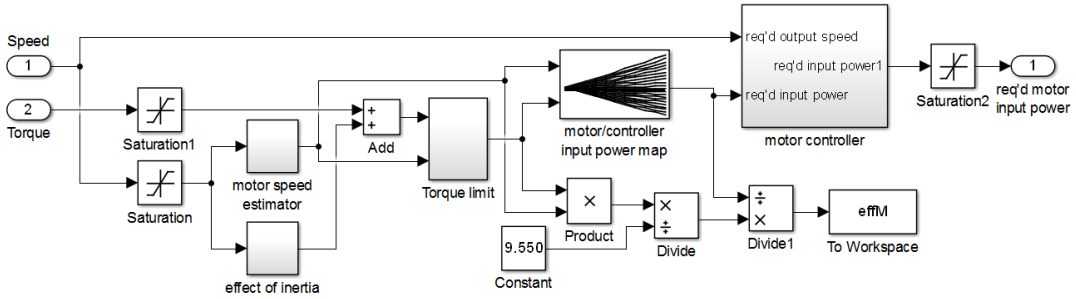

Fig. 17. Spindle motor simulation model

The motor efficiency is calculated to demonstrate the improvement on the energy efficiency. Different working conditions are set as input of the simulation model according to Fig. 14 and Fig. 15. The motor efficiency for camshaft and input shaft are given by Fig. 18a and Fig. 18b, respectively. It is clear from Fig. 18 that the efficiency of optimized spindle motor has been improved at most working point, resulting in the reduction of energy consumption in the machining process.

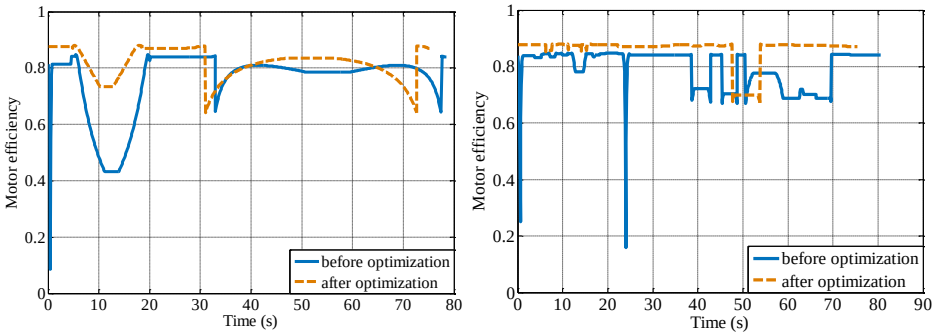

(a) (b)

Fig. 18. Spindle motor efficiency for machining a) camshaft and b) input shaft

(4) Energy consumption monitor model

The input power of spindle system is computed through motor efficiency and output power obtained from spindle motor model. The energy consumption of spindle system can be calculated as the integral of input power and processing time, which can be obtained through energy consumption monitor model. Fig. 19a and Fig. 19b show the accumulation process of energy consumption when machining camshaft and input shaft. It is clear from Fig. 19 that the energy consumption is reduced to some extent through design optimization of spindle system. The comparison results of energy consumption are shown in Table 7. The energy consumed by machining a camshaft is reduced from 1.5035E5J to 1.3543E5J (with 9.92% energy reduction), while the energy consumed by machining an input shaft is reduced from 1.4471E5J to 1.2710E5J (with 12.17% energy reduction). Due to the improvement of the motor efficiency at working times, the energy consumption of the spindle system during machining process is reduced.

Table 7. Optimization results of energy consumption

Workpiece	Objective	Before optimization	After optimization	Reduction
Camshaft	Energy consumption E_{sp}(J)	1.5035E5	1.3543E5	9.92%
Input shaft	Energy consumption E_{sp}(J)	1.4471E5	1.2710E5	12.17%

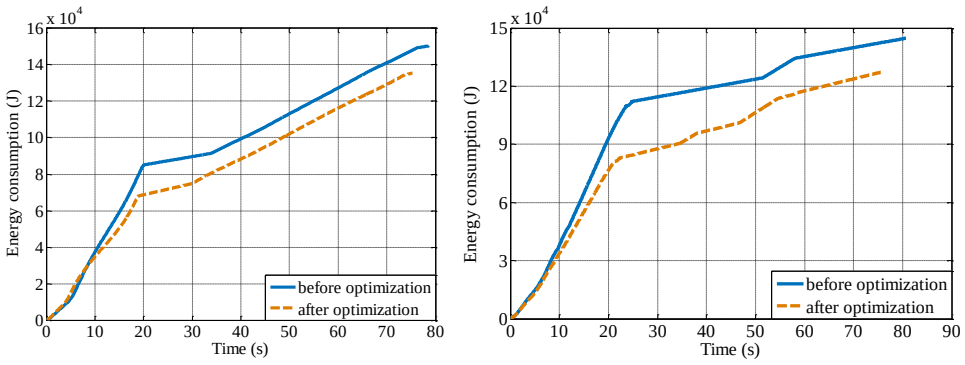

(a) (b)

Fig. 19. Energy consumption curves for machining a) camshaft and b) input shaft

5 Conclusions

The improvement of both the energy and the material efficiency of spindle system is of great significance to enhance the sustainability performance of machine tools. This paper presents a design optimization method for the spindle system by integrated optimization of spindle motor and transmission system parameters. The energy models of spindle systems are developed on the basis of the energy flows between spindle motors and transmission systems. A multi-objective optimization model is formulated for parameter settings of spindle motor and transmission system with an objective to minimize the specific energy consumption and minimize the structure volume. Then, the MO-ITLBO algorithm is proposed to find Pareto optimal solutions for the integrated optimization problem. Case studies are conducted to verify the performance of the proposed multi-objective optimization approach. The experimental results showed that the multi-objective optimization model can achieve a trade-off between minimum specific energy consumption and minimum structure volume. Moreover, the optimization results have been proved to be effective in reducing energy consumption.

Based on this study, future work will be concentrated on exploring the interactions between various design and performance parameters. In addition to the driving parameters of the spindle motor and transmission system, the structure parameters of the spindle shaft affect the design of spindle system. Thus, introducing structure parameters into the design optimization can be further explored.

Acknowledgements

This work was supported in part by the National Natural Science Foundation of China under Grant 51975075, in part by the Chongqing Technology Innovation and Application Program under Grant cstc2018jszx-cyzdX0146, and in part by the Fundamental Research Funds for the Central Universities of China under Grant cqu2018CDHB1B07.

References

Al-Badri, M., Pillay, P., Angers, P., 2015. A Novel In Situ Efficiency Estimation Algorithm for Three-Phase IM Using GA, IEEE Method F1 Calculations, and Pretested Motor Data. IEEE. T. Energy. Conver. 30(3), 1092-1102. https://doi.org/10.1109/TEC.2015.2421288.

Armarego, E.J.A., Ostafiev, D., Wong, S.W.Y., Verezub, S., 2000. An appraisal of empirical modeling and proprietary software databases for performance prediction of machining operations. Mach. Sci. Technol. 4(3), 479-510. https://doi.org/10.1080/10940340008945719.

Chakkarapani, K., Thangavelu, T., Dharmalingam, K., Thandavarayan, P., 2019. Multiobjective design optimization and analysis of magnetic flux distribution for slotless permanent magnet brushless DC motor using evolutionary algorithms. J Magn. Magn. Mater. 476, 524-537. https://doi.org/10.1016/j.jmmm.2019.01.029.

Chen, X.Z., Li, C.B., Tang, Y., Li, L., Du, Y.B., Li, L.L., 2019. Integrated optimization of cutting tool and cutting parameters in face milling for minimizing energy footprint and production time. Energy. 175, 1021-1037. https://doi.org/10.1016/j.energy.2019.02.157.

Diez-Ibarbia, A., del Rincon, A.F., Iglesias, M., de-Juan, A., Garcia, P., Viadero, F., 2016. Efficiency analysis of spur gears with a shifting profile. Meccanica. 51(3), 707-723. https://doi.org/10.1007/ s11012-015-0209-x.

Gutowski, T., Dahmus, J., Thiriez, A., 2006. Electrical energy requirements for manufacturing processes. In: Processings of 13th CIRP international conference on life cycle engineering, Leuven, Belgium. 5-11.

Golabi, S., Fesharaki, J.J., Yazdipoor, M., 2014. Gear train optimization based on minimum volume/weight design. Mech. Mach. Theory. 73, 197-217. https://doi.org/10.1016/ j.mechmachtheory.2013.11.002.

Hall, E., Ramamurthy, S.S., Balda, J.C., 2001. Optimum Speed Ratio of Induction Motor Drivers for Electric Vehicle Propulsion. APEC, Anaheim. https://doi.org/10.1109/ APEC.2001.911674

ISO, 2017. 14955-1: Machine tools - Environmental evaluation of machine tools - Part 1: Design methodology for energy-efficient machine tools. https://www.iso.org/standard/70035.html.

IEA, 2017, World Energy Balances: Overview, International Energy Agency, Paris, France, accessed Dec. 20, 2017, http://www.iea.org/publications/freepublications/publication/ WorldEnergyBalances2017Overview.pdf.

Li, C.B., Li L.L., Tang, Y., Zhu, Y.T., Li, L., 2019. A comprehensive approach to parameters optimization of energy-aware CNC milling. J. Intell. Manuf. 30(1), 123-38. https://doi.org/10.1007/s10845-016-1233-y.

Liu, F., Xie, J., Liu, S., 2015. A method for predicting the energy consumption of the main driving system of a machine tool in a machining process. J. Clean. Prod. 105, 171-177. https://doi.org/ 10.1016/ j.jclepro.2014.09.058.

Liu, P.J., Liu, F., Liu, G.J., 2017. A new approach for calculating the input power of machine tool main transmission systems. Adv. Mech. Eng. 9(9), 1-10. https://doi.org/10.1177/ 1687814017723791.

Liu, S., Liu, F., Hu, S.H., Yin, Z.B., 2012. Energy Survey of Machine Tools: Separating Power Information of the Main Transmission System During Machining Process. J. Adv. Mech. Des. Syst. 6(4), 445-455. https://doi.org/10.1299/jamdsm.6.445.

Liu, Z.Y., Sealy, M.P., Li, W., Zhang, D., Fang, X.Y., Guo, Y.B., Liu, Z.Q., 2018. Energy consumption characteristics in finish hard milling. J. Manuf. Process. 35, 500-507. https://doi.org/10.1016/ j.jmapro.2018.08.036.

Lv, J.X., Tang, R.Z., Tang, W.C.J., Liu, Y., Zhang, Y.F., Jia, S., 2017. An investigation into reducing the spindle acceleration energy consumption of machine tools. J. Clean. Prod. 143, 794-803. https://doi.org/10.1016/j.jclepro.2016.12.045.

Miler. D., Zezelj, D., Loncar, A., 2018. Multi-objective spur gear pair optimization focused on volume and efficiency. Mech. Mach. Theory. 125, 185-195. https://doi.org/10.1016/ j.mechmachtheory.2018.03.012.

Mendi, F., Başkal, T., Boran, K., Boran, F. E., 2010. Optimization of module, shaft diameter and rolling bearing for spur gear through genetic algorithm. Expert. Syst. Appl. 37(12), 8058-8064. https://doi.org/10.1016/j.eswa.2010.05.082.

Nejadkhaki, H.K., Chaudhari, S., Hall, J.F., 2018. A design methodology for selecting ratios for a variable ratio gearbox used in a wind turbine with active blades. Renew. Energ. 118, 1041-1051. https://doi.org/ 10.1016/j.renene.2017.10.072.

Patel, V.K., Savsani, V.J., 2016. A multi-objective improved teaching–learning based optimization algorithm (MO-ITLBO). Inform. Sciences. 357, 182-200. https://doi.org/10.1016/ j.ins.2014.05.049.

Rao, R.V., Savsani, V.J., Vakharia, D.P., 2011. Teaching-learning-based optimization: A novel

method for constrained mechanical design optimization problems. Comput. Aided. Design. 43(3), 303-315. https://doi.org/10.1016/j.cad.2010.12.015.

Waide, P., Brunner, C.U., 2011. Energy-Efficiency Policy Opportunities for Electric Motor-Driven Systems. IEA, Paris. https://doi.org/10.1787/5kgg52gb9gjd-en.

Wójcicki, J., Bianchi, G., 2018. Electric load management in spindle run-up and run-down for multi-spindle machine tools via optimal power-torque trajectories and peak load synchronization. Int. J. Adv. Manuf. Tech. 95(5-8), 1819-1835. https://doi.org/10.1007/ s00170-017-1341-7.

Wang, H., Zhong, R. Y., Liu, G., Mu, W., Tian, X., Leng, D., 2019. An optimization model for energy-efficient machining for sustainable production. J. Clean. Prod. 232, 1121-1133. https://doi.org/10.1016/j.jclepro.2019.05.271.

Xiao, Q.G., Li, C.B., Tang, Y., Li, L.L., Li, L., 2019. A knowledge-driven method of adaptively optimizing process parameters for energy efficient turning. Energy. 166, 142-156. https://doi.org /10.1016/j.energy.2018.09.191.

Xiao, Q.G., Li, C.B., Tang, Y., Li, L.L., 2019. Meta-reinforcement learning of machining parameters for energy-efficient process control of flexible turning operation. IEEE T. Autom. Sci. Eng. https://doi.org/ 10.1109/TASE.2019.2924444.

Xie, J., Liu, F., Qiu, H., 2016. An integrated model for predicting the specific energy consumption of manufacturing processes. Int. J. Adv. Manuf. Tech. 85(5-8), 1339-1346. https://doi.org/ 10.1007/s00170-015-8033-y.

Zhang, J., Qin, X., Xie, C., Chen, H., Jin, L., 2018. Optimization design on dynamic load sharing performance for an in-wheel motor speed reducer based on genetic algorithm. Mech. Mach. Theory. 122, 132-147.

Zhu, X.Y., Fan, D.Y., Xiang, Z.X., Quan, L., Hua, W., Cheng, M., 2019. Systematic multi-level optimization design and dynamic control of less-rare-earth hybrid permanent magnet motor for all-climatic electric vehicles. Appl. Energy. 253, 113549. https://doi.org/10.1016/ j.apenergy.2019.113549